Stem Cell Reports, Volume *9*

Supplemental Information

Mouse Genetic Analysis of Bone Marrow Stem Cell Niches: Technological Pitfalls, Challenges, and Translational Considerations

Kevin G. Chen, Kory R. Johnson, and Pamela G. Robey

Table S1. Developmental Stage-Related Marker Gene Expression in Bone Marrow Stem Cell Lineages: Conditions and Constrains in Murine Models

Stages	Mouse strains/cells	Major findings & descriptions	CFU-F	Authors' comments	References
E8.5-, E10.5-, E18.5	*Nes*-CreER^{T2}: RCE-loxP	Tamoxifen induction at E8.5 & E10.5, chase to E18.5: *Nes*-Cre^{+} cells, not found in proliferating and hypertrophic chondrocytes, infiltrate over osteochondral junction and into the trabecular bone.	0.8%	BM *Nes*-Cre^{+} cells do not contribute to fetal endochondrogenesis.	(Isern et al., 2014)
E9.5	*Sox10*-CreER^{T2}	Among 18% of Sox10-Cre^{+} cells, 72% of them were *Nes*-GFP^{+}/PDGFRα^{+} cells.	NA	Evidence of *Nes*-GFP^{+} cells' neural crest association	(Isern et al., 2014)
E10.5	*Nes*-GFP^{+}/ CD31^{+} cells	Represent 8% of endothelial cells at limb buds	NA	Appeared at the endochrondral condensation stage	(Ono et al., 2014)
E11.5	*Nes*-GFP^{+}/ CD31^{+} cells	Observed at the perichondrium	NA	*Nes*-GFP^{+} cells are rarely found within the mesenchymal condensation region.	(Ono et al., 2014)
E11.5-P0, P21	*Nes*-CreER^{T2}: Rosa26 tomato	Tamoxifen induction (from E11.5) before the formation the POC and chase to P0 and P21: only few *Nes*-Cre^{+} cells found in bone at P0 and P21	NA	After the POC, *Nes*-Cre^{+} cells do not commit to neonatal and postnatal bone development.	(Ono et al., 2014)
E12.5	*Nes*-GFP^{+} /CD31^{-} cells	1st appearance at the perichondrium	NA	None	(Ono et al., 2014)
E13.5	*Nes*-GFP^{+} /CD31$^{+/-}$ cells	►Overlap with Col2^{+} cells at the perichondrium ►Some *Nes*-GFP^{+} cells are likely derived from collagen II-expressing (chondrogenic) cells. ►Perichondral *Nes*-GFP^{+}CD31$^{+/-}$ cells are regulated by both Ihh and Runx2.	NA	*Nes*-GFP^{+}/CD31^{-} non-endothelial cells become osteoprogenitor cells upon Ihh and Runx2 induction.	(Ono et al., 2014)
E13.5	*Nes*-CreER^{T2}: RCE-loxP	Similar to *Nes*-GFP^{+} cells: detected near the chondral–perichondral interface and the osteo-chondral junction	NA	Consistent with the dynamic nature of *Nes*-GFP^{+} cells	(Isern et al., 2014)
E13.5-P0, P21	*Nes*-CreER^{T2}: Rosa26 tomato	Tamoxifen induction and chase from E13.5: only few *Nes*-Cre^{+} cells found in bone at P0 and P21	NA	After the POC, *Nes*-Cre^{+} cells do not commit to neonatal and postnatal bone development.	(Ono et al., 2014)
E14.5	*Nes*-GFP^{+} /CD31$^{+/-}$cells	Both types of *Nes*+ cells occupied at the inner perichondrium, with *Nes*-GFP^{+} /CD31^{-} cells aligned on the innermost portion.	NA	None	(Ono et al., 2014)
E15.5	*Nes*-GFP^{+} /CD31$^{+/-}$ cells	►Infiltrate into the cartilage template along vascular invasion ►Increase in *Nes*-GFP^{+}/CD31$^{+/-}$ cell numbers ►*Nes*-GFP^{+}CD31$^{+/-}$ closely associated at the POC	NA	*Nes*-GFP^{+}/CD31^{+} cells show (at least 3-fold) stronger GFP signals than *Nes*-GFP^{+}/CD31^{-} cells at E15.5, suggesting that *Nes*-GFP transcription is positively regulated by endothelial cell signaling.	(Ono et al., 2014)
E15.5	*Lepr*-Cre	Absence of *Lepr*-Cre^{+} cells at the POC at this stage		*Nes*-GFP^{+} and *Osx*-Cre^{+} emerged in the POC	(Mizoguchi et al., 2014)
E15.5	*Nes*-creER^{T2}: iDTR mice	Deletion of *Nes*-Cre^{+} cells in this double transgenic mice resulted in 4-fold decrease in HSC activity in fetal BM within 48 hours, concomitantly with 8-fold increase in HSCs in fetal liver	NA	These data suggest that *Nes*-GFP transcriptome positively regulates the migration of HSC niches from the embryonic liver to the BM.	(Isern et al., 2014)
E16.5-P7, P21	*Nes*-CreER^{T2}: *Rosa26 tomato*	Tamoxifen induction at E16.5, the time that the marrow space starts to form, and chase to P7 and P21: see larger numbers of *Nes*-Cre^{+} in bone	0.3%,	*Nes*-CreER transcription is repressed before the formation of POC, but derepressed after the formation of the POC and marrow cavity.	(Ono et al., 2014)
E17.5	*Lepr*-Cre^{+} cells	►1st appearance of *Lepr*-Cre^{+} cells ►Found in the primary spongiosa and the periosteum	NA	*Lepr*-Cre^{+} cells in the periosteum might be originated from *Nes*-GFP^{+}/CD31$^{+/-}$ cells as described by Ono et al. 2014.	(Mizoguchi et al., 2014)
E17.5	*Nes*-GFP^{+} cells	Display 3-fold lower CFU-Fs than *Nes*-GFP^{-} cells, but higher capacity to form "mesenspheres"	0.1%	Higher SCC potential in *Nes*-GFP^{+} cells than *Nes*-GFP^{-} cells	(Isern et al., 2014)

E17.5	*Nes*-GFP$^+$ cells	Not associated with *Col2.3*-Cre$^+$ cells and chondrocytes	0.1%	Distinction from osteoblastic cells	(Isern et al., 2014)
E18.5	*Nes*-GFP$^+$ cells	Frequently associated with arterioles and nascent CD31$^+$ endothelial cells within the osteochondral junction; but not with osterix (by antibody staining);	0.8%	►Express endogenous *Nes* mRNAs at this stage ►CFU-F frequency 6-fold lower than *Nes*-GFP$^-$ cells	(Isern et al., 2014)
E18.5-P1, Peri-natal	*Nes*-GFP$^+$ cells	►*Nes*-GFP$^+$ cells, likely derived from neural crest ►Secrete the HSC niche factor Cxcl12 ►Distinguished from mesoderm derived "MSCs" ►Do not generate fetal chondrocytes	0.2%	►Perinatal stages: from E18.5 to postnatal day 1 (www.jax.org) ► "MSCs" are an incorrect terminology that depicts BM SSCs.	(Isern et al., 2014)
E19.5	*Lepr*-Cre: dTomato; Col2.3-GFP	*Lepr*-Cre$^+$ cells were rare and had no contribution to bone development at this stage.	NA	Used for explicitly identifying osteoblastic bone-lining cells	(Zhou et al., 2014)
P0	*Nes*-GFP$^+$ cells	Belong to BM CD45$^-$/CD31$^-$/Ter119$^-$ stromal cells	0.2%	P0, neonatal stage	(Isern et al., 2014)
P0	*Nes*-GFP$^+$ /PDGFRα^- cells	►*Nes*-GFP$^+$ cells are close to HSCs (within 20 µm) in the neonatal BM. ►Express mRNAs (e.g., *Sox10*, *Plp1*, *Erbb3*, and *Dhh*), typically presented in Schwann cell precursors ►No *Gfap* found in mature Schwann cells	0.2%	►Give rise to distinct HSC niche-forming stromal cells *in vivo* ►Have a high glial differentiation propensity *in vitro*	(Isern et al., 2014)
P0	*Nes*-GFP$^+$ /PDGFRα^+ cells	►Enriched mRNA transcripts associated with HSC niche maintenance genes (e.g. *Cxcl12*, *KitL*, *Angpt1*, and *Lepr*), may have a role in HSC maintenance ►Have an *in vitro* mesodermal (adipocyte) differentiation propensity	0.2%	►*Nes*-GFP$^+$ cells show physical proximity to the HSC niche. ►Osteoblastic differentiation genes were selectively inhibited during enforced HSC mobilization or Adrb3 activation (Mendez-Ferrer et al. 2010).	(Isern et al., 2014)
P0.5	*Lepr*-Cre: dTomato: *Col2.3*-GFP	►A drastic increase in the number of *Lepr*-Cre$^+$ cells in metaphysis ►The emergence of few *Lepr*-Cre$^+$/Col2.3-GFP$^+$ osteoblasts in trabecular bone	NA	This probably is the earliest osteogenic contribution made by *Lepr*-Cre$^+$ cells, highlighting the 1st plausible postnatal SSC niche at the metaphyseal and trabecular regions.	(Zhou et al., 2014)
P0-P7	*Nes*-CreER^{T2}	Tamoxifen induction at P0 and chase to P7: highly colocalized with BM *Nes*-GFP$^+$ cells	0.3%	Two transcriptional mechanisms for *Nes*-GFP are consistent at this stage, suggesting the two reporter systems might share an enhancer complex at the intron 2 of the *Nes* gene.	(Isern et al., 2014)
P0-P14	*Nes*-GFP: *Nes*-CreER^{T2}	Tamoxifen induction at the neonatal stage (P0): *Nes-GFP*$^+$ cells overlap with *Nes*-CreER^{T2+} cells.	0.3%	It appears that *Nes*-Cre$^+$ cells partially overlay with *Nes-GFP*$^+$ cells at BM blood vessels, but not in *Nes*-GFP$^+$ perivascular pericytes.	(Isern et al., 2014)
P3	*Nes*-GFP$^+$ cells	CFU-F activity much lower than *Nes*-GFP$^-$ cells	0.3%	None	(Isern et al., 2014)
P3	*Nes*-GFP: *Tie2*-Cre	94% *Nes*-GFP$^+$/*Tie2*-Cre$^+$/CD45$^-$ cells	NA	*Nes*-GFP$^+$ cells have a role in specifying endothelial cells.	(Ono et al., 2014)
P3-P5	*Nes*-GFP: *Nes*-CreER^{T2}	Tamoxifen induction at P3 and chase to P5: ►Almost 100% *Nes*-GFP$^+$/*Nes*-Cre$^+$ cells ►81% *Nes*-Cre$^+$/CD31$^+$ cells at the primary spongiosa and BM ►34% *Nes*-GFP$^+$/CD31$^+$ endothelial cells ►*Nes*-GFP$^+$/*Nes*-CreER$^+$ cells also express endogeneous *Nes* mRNAs and the nestin protein (detected by flow cytometry using ab6142). ►*Nes* mRNA (by quantitative PCR) increased by 82-, 263-, and 414-fold in *Nes*-GFP$^+$/*Nes*-Cre$^-$CD31$^-$, *Nes*-GFP$^+$/*Nes*-Cre$^-$CD31$^+$, and *Nes*-	NA	►*Nes*-Cre is inducible at 48 hours after tamoxifen administration ►Both *Nes*-GFP$^+$ and *Nes*-Cre$^+$ cells likely share a transcriptional mechanism at this stage. ►*Nes*-Cre transcriptional activity is dominant over *Nes*-GFP in CD31$^+$ endothelial cells. ►Additional transcriptional activators from endothelial cells are needed to drive endogenous *Nes* mRNA expression to a high level.	(Ono et al., 2014)

		GFP$^+$/*Nes*-Cre$^+$, respectively, relative to *Nes*-GFP negative control			
P3-P5, P10, P17, P24, 4w	*Nes*-creER^{T2}: Rosa26 tomato: Col1(2.3kb)-GFP	Tamoxifen induction at P3 and chase up to 1 month (4 weeks or 4w): ►10% *Nes*-Cre$^+$ osteoblasts expressing Col1 at P5 ►*Nes*-Cre$^+$ cells increased up to 26% and 23% at P10 and P17 respectively ►*Nes*-Cre$^+$ decreased to 5% and 3% at P24 and 4w respectively	NA	*Nes*-Cre$^+$ cells have limited contribution to osteoblasts at the postnatal stage (within one month).	(Ono et al., 2014)
P3-P10	*Nes*-GFP: *Osx*-CreER	Tamoxifen induction at P3 and chase to P10: 96% of cells targeted by *Osx*-CreER were positive for *Nes*-GFP (i.e. *Nes*-GFP$^+$/*Osx*-CreER$^+$).	NA	*Nes*-GFP$^+$ cells might have a major role in specifying osteoblasts at this stage.	(Ono et al., 2014)
P3-P10	*Nes*-GFP: *Col1*(3.2kb)-CreER	Tamoxifen induction at P3 and chase to P10: 92% *Nes*-GFP$^+$/*Col1*(3.2kb)-CreER$^+$	NA	The same comment as above	(Ono et al., 2014)
P3-P10	*Nes*-GFP: *Ocn*-CreER	Tamoxifen induction at P3 and chase to P10: 93% *Nes*-GFP$^+$/*Ocn*-Cre$^+$	NA	The same comment as above	(Ono et al., 2014)
P3-24w	*Nes*-CreER^{T2}: Rosa26 tomato	Tamoxifen induction at P3 and chase 6 months (24 weeks or 24w): ►*Nes*-Cre$^+$ cells distributed from the BM to the growth plate; 84% *Nes*-CreER$^+$ /CD31$^+$ cells; ►*Nes*-Cre$^+$ descendant cells form reticular sinusoidal endothelial cells for at least 24 weeks. ►*Nes*-Cre$^+$ cells generate few osteoblasts, osteocytes, and chondrocytes; but no adipocytes	NA	In adult BM, *Nes*-Cre$^+$ cells mainly contribute to sinusoidal endothelial cells.	(Ono et al., 2014)
P5-P6	*Nes*-GFP: iOsx/Tomato	Tamoxifen induction at P5 and chase to P6: ~38% of iOsx$^+$ cells were *Nes*-GFP$^+$ in bone tissues.	NA	P5-iOsx$^+$ BM cells exhibit a trilineage differentiation potential.	(Mizoguchi et al., 2014)
P5-4w	iOsx/Tomato	Tamoxifen induction at P5: increased CFU-F frequency of sorted iOsx/Tomato$^+$ cells in the BM stroma harvested at 4 weeks after tamoxifen injection	0.5% at 4w	None	(Mizoguchi et al., 2014)
P5-15w	*Nes*-GFP: iOsx/Tomato;	Tamoxifen induction at P5 and chase to 15w in CD45$^-$/Ter119$^-$/CD31$^-$/iOsx$^+$ BM stromal cells: 78% *Nes*-GFP$^+$/Lepr$^+$ (using anti-Lepr), in which 89% of cells were PDGFRα^+ and 83% of cells PDGFRβ^+	NA	►Regulation of *Nes*-GFP and *Lepr* is converged at this stage, apparently for the maturation of bone development. ►No Western blots used to define the size of the Lepr protein in this and other studies.	(Mizoguchi et al., 2014)
P5-15w, 16w, 19w	*Lepr*-Cre: *Osx*-Cre /Tomato	*Osx*-Cre/Tomato mice pulsed at P5 and fracture wound started in 15w-old *Lepr*-Cre/Tomato mice: ►Observed freshly made chondrogenic zones of the fracture callus at day 8 (total 16w) ►No *Osx*-Cre$^+$ chondrocytes observed after 3w chase (total 19w)	NA	See comments to P5-32w below.	(Mizoguchi et al., 2014)
P5-32w-33w	*Lepr*-Cre: *Osx*-Cre /Tomato	Osx-Cre/Tomato mice pulsed at P5 and fracture wound started in 32w-old mice: ►Some *Lepr*-Cre$^+$ cells, identified as Sox9$^+$ cells in the fractured callus, contributed to progenitors of osteocytes, chondrocytes, and adipocytes *in vivo*. ►*Lepr*-Cre+ cells not colocalized well with the Lepr protein in the non-fracture callus region ►No Lepr protein detected (by an antibody from R&D Systems) in the fracture callus at day 8 (33w)	NA	These data suggest the Lepr protein is not required for the skeletal repair, thus reinforcing the role of *Lepr* transcriptomes as pivotal indicators of skeletal development.	(Mizoguchi et al., 2014)
P7	*Nes*-GFP$^+$	~2.4-fold decrease in *Nes* mRNAs relative	0.3%	Evidence of a dynamic *Nes*	(Isern et al.,

	cells	to E18.5		transcriptome	2014)
P7	*Lepr*-Cre$^+$ cells	►Distributed throughout the BM cavity ►~92% *Lepr*-Cre$^+$ cells also positive for *Nes*-GFP in the BM ►Positive for *Nes*-GFP and *Osx*-Cre in the primary spongiosa	NA	The emergence of *Lepr*-Cre dominance (in the developing bone and BM) coincides with the decrease of *Nes*-GFP transcriptional activity, suggesting a coordinate regulation between the *Lepr* and *Nes* genes.	(Mizoguchi et al., 2014)
P7	Gfap$^+$ cells	Schwann cells expressing Gfap detected in the BM	0.3%	Gfap: a marker for non-myelin-forming Schwann cells	(Isern et al., 2014)
P7	*Nes*-GFP: *Wnt1*-Cre2	Increase in *Wnt1*-Cre2-traced osteochondral cells; partially overlap with *Nes*-GFP$^+$ cells, including perivascular *Nes*-GFP$^+$ cells	0.3%	Wnt1 is not a specific marker for neural crest cells.	(Isern et al., 2014)
P7	*Nes*-GFP	►*Nes*-GFP$^+$ cells distributed at the diaphysis and metaphysis (close to the growth plate) in endochondral bones ►*Nes*-GFP^{high} cells traced perivascular cells in the primary spongiosa and pericytes of the arterioles in diaphysis ►*Nes*-GFP^{low} cells in osteoblasts on the bone surface, osteocytes, and endothelial cells	NA	See comments on *Nes*-GFP expression at 8w described by Ono et al., 2014	(Ono et al., 2014)
P7	*Nes*-GFP: *Lepr*-Cre	97% *Nes*-GFP$^+$/*Lepr*-Cre$^+$/CD45$^-$ cells	NA	*Nes*-GFP$^+$ cells may have a role in specifying *Lepr*-Cre$^+$ SSCs.	(Ono et al., 2014)
P7	*Nes*-GFP: Osx-Cre	98% *Nes*-GFP$^+$/*Osx*-Cre$^+$/CD45$^-$ cells	NA	*Nes*-GFP$^+$ cells are associated with osteoblast development.	(Ono et al., 2014)
P7 & more stages	*Mx1-Cre*	►*Mx1*-Cre labels non-hematopoietic and non-endothelial osteogenic cells in the bone. ►*Mx1-Cre*$^+$ cells are highly enriched at the postnatal day 7. ►*Mx1-Cre*$^+$ cells are resided at the perivascular niche and enriched in the CD105$^+$/CD140a$^+$ subset (43%) and calvarial sutures. ►59% *Nes*-GFP$^+$ cells overlap with *Mx-1*$^+$ cells. ►*Mx1*-Cre$^+$ stromal cells are lineage-restricted, essential for supplying new osteoblasts, and for fracture healing *in vivo*. ► *Mx1*-Cre$^+$ cells are clonogenic, having tripotent differentiation potential *in vitro* and *in vivo*. ► *Mx1*-Cre labels mature osteogenic cells that express osterix, osteopontin, and osteocalcin.	High	►*Nes*-GFP$^+$ cells may be the precursor of *Mx1*-cre$^+$ cells. ►*Mx1*-Cre$^+$ cells may contribute to pre-osteoblasts. ►No chondrogenesis is required for adult bone fracture repair. ►*Mx1*-Cre-labeled cells partially overlap with nestin$^+$ cells detected by an anti-nestin antibody (Millipore, clone rat-401). ►*Mx1*-Cre can be used to distinguish long-term osteogenic cells from other bone-forming cells. ►The osteoblastic turnover rates vary at different developmental stages.	(Park et al., 2012)
P14	*Nes*-GFP$^-$ cells	More than 100-fold decrease in CFU-F activity in *Nes*-GFP$^-$ BM stromal cells compared with E18.5 cells	~0%	Unknown mechanisms to regulate this critical transition	(Isern et al., 2014)
P21	*Nes*-GFP$^+$ cells	Maintain steady CFU-F activity	0.3%	None	(Isern et al., 2014)
P21	*Lepr*-Cre$^+$ cells	Distributed throughout the BM cavity, but not on the endosteum	NA	See comments on *Lepr*-Cre$^+$ cells at 15w	(Mizoguchi et al., 2014)
P28	*Wnt1*-Cre2$^+$ cells	CFU-F activity was much higher in *Wnt1*-Cre2$^+$ cells than in *Wnt1*-Cre2$^-$ BM stromal cells.	0.2%	See above comments.	(Isern et al., 2014)
5w	*Nes*-GFP	*Nes*-GFP$^+$ cells clustered, but not colocolized, with osterix$^+$ cells (by immunostaining) in trabecular bone sections	NA	None	(Mendez-Ferrer et al., 2010)
7w-12w	*Nes*-GFP^{high} cells	►Exceptionally low, 0.002% of BM cells ►Quiescent, only along arterioles ►NG2$^+$ and α-smooth muscle actin$^+$	High	►Likely have an HSC-niche-supporting role ►Neither *Nes*-GFP^{high} nor *Nes*-	(Kunisaki et al., 2013)

		pericytes ►Physically associated with tyrosine hydroxylase (HT) positive sympathetic nerves and GFAP$^+$ Schwann cells ►Do not overlap with *Lepr*-Cre$^+$ cells		GFP^{low} BM stromal cells seem to express endogenous *Nes* mRNAs by microarray (Mendez-Ferrer et al., 2010) and by RNA sequencing (Kunisaki et al., 2013).	
7w-12w	*Nes*-GFP^{low} cells	Abundant, reticular in shape, mainly associated with perisinusoids and overlap with *Lepr*-Cre$^+$ cells	Low	Likely pericytes for SSCs	(Kunisaki et al., 2013)
7w-12w	*Nes*-GFP^{high} /*Lepr*-Cre$^-$ cells	►*Nes*-GFP^{high}/*Lepr-cre*$^-$ cells express the highest level of *Scf* and *Cxcl12*. ►RNA-seq data showed that *Nes*-GFP^{high}/*Lepr-cre*$^-$ cells were negative for *Nes* and positive for *Lepr* expression (GSE48764).	NA	►Discrepancy between transcriptome and transcriptional activity ►Evidence of a putative inverse regulation between the *Nes* and *Lepr* genes	(Kunisaki et al., 2013)
7w-12w	*Nes*-GFP: *NG2*-CreER	*Nes*-GFP^{high} cells (~30%), not *Nes*-GFP^{low} cells, colocalized with *NG2*-Cre$^+$ cells	NA	None	(Kunisaki et al., 2013)
7w-12w	*NG2*-CreER: iDTR	►Tamoxifen induction and diphtheria toxin treatment depleted ~55% of *Nes*-GFP^{high} cells. ►Depletion of NG2$^+$ cells expelled quiescent HSCs from arteriolar to perisinusoidal niches.	NA	*NG2*-Cre$^+$ cells are believed to be part of HSC niches, which endorses HSC for quiescence.	(Kunisaki et al., 2013)
8w	*Nes*-GFP	In endochondral bones: ►*Nes*-GFP^{high} cells were decreased in the primary spongiosa and BM. ►*Nes*-GFP^{low} cells were further decreased in osteoblasts (on bone surfaces), osteocytes, but still observable at this stage.	NA	From P7 to 8w, *Nes*-GFP$^{high/low}$ cells continue to decrease without a conclusive mechanism.	(Ono et al., 2014)
8w	*Lepr*-Cre$^+$ /*Col2.3*-GFP$^-$	*Lepr*-Cre$^+$/*Col2.3*-GFP$^-$/CD45$^-$/Ter119$^-$ /CD31$^-$ BM cells ►Cell frequency stabilized near 0.2% ►Quiescent at 8w, reactivable under stress conditions ►Intrafemoral injection of 500 of these cells generated adipocytes, osteocytes, and chondrocytes at 4w.	NA	These data suggest that *Lepr*-Cre$^+$/*Col2*.3-GFP$^-$ cells are a progenitor cell source for adipocytes and osteolineage cells.	(Zhou et al., 2014)
8w	*Nes*-CreER^{T2}: *Scf*$^{fl/-}$	Deletion of Scf from *Nes*-Cre$^+$cells did not affect HSC frequency in BM.	NA	HSC niche maintenance does not require SCF from *Nes*-Cre$^+$ cells.	(Ding and Morrison, 2013)
8w	*Nes-GFP*	*Nes*-GFP^{high} along larger vessels in BM; *Nes*-GFP^{low} in perisinusoidal stromal cells similar to *Scf*-GFP$^+$ cells	NA	*Nes*-GFP expression patterns in this study are consistent with the report by Mendez-Ferrer et al. 2010.	(Ding and Morrison, 2013)
8w	*Nes-Cre*$^+$ *cells*	Only found around larger blood vessels in BM	NA	*Nes* expression discrepancies	(Ding and Morrison, 2013)
8w	*Nes-Cherry: Nes-GFP*	*Nes-Cherry*$^+$ cells were around larger vessels but not around sinusoids, whereas *Nes*-GFP$^+$ cells were detected around both regions.	NA	*Nes*-Cherry has a similar expression pattern to that of *Nes*-Cre. However, the detail information about *Nes*-Cherry mice is not available.	(Ding and Morrison, 2013)
8w (2m)	*Lepr*-Cre: dTomato: *Col2.3*-GFP	*Lepr*-Cre$^+$ cells were filled with metaphysis and diaphysis of the BM,	NA	The emergence of 3-10% *Lepr*-Cre$^+$/*Col2.3*-GFP$^+$ osteoblasts in bone	(Zhou et al., 2014)
8w-16w	*Wnt1*-CreER	*Wnt1*-CreER$^+$/CD45$^-$/Ter119$^-$ BM stromal cells	0.5%	*Wnt1*-Cre$^+$ neural crest derivatives minimally contribute to CFU-F colonies at this stage.	(Zhou et al., 2014)
8w-12w	*Nes*-GFP: Lepr	70% of Lepr$^+$ cells (by flow cytometric analysis) in BM mainly overlap with *Nes*-GFP$^+$ cells.	NA	None	(Pinho et al., 2013)
8w-12w	PDGFRα^+ /CD51$^+$	PDGFRα^+/CD51$^+$ cells represent a small subset of *Nes*-GFP$^+$ cells. *Nes* mRNAs are expressed in this cell population.	NA	Expression of CD51 (the integrin subunit αV) enhances *Nes* mRNA expression and might enable to convert *Nes*-GFP$^+$/PDGFRα^+	(Pinho et al., 2013)

				/CD146$^+$ cells into perivascular pericytes.	
8w-12w	α-catulin-GFP$^+$ cells	►Represent 0.02% of BM hematopoietic cells, located at the central perisinusoids ►Restricted to HSC niche cells, adjacent to *Lepr*$^+$ and Cxcl12$^+$ cells, ►Distant from arterioles and endosteal surface ►HSCs located within the 10 μm sinusoidal vessels with an HSC frequency of 1/6	NA	These data are inconsistent with periarteriolar HSC-niches supported by *NG2*–CreER$^+$ cells in a previous report (Kunisaki et al. 2013).	(Acar et al., 2015)
8w-12w	Gfap$^+$ cells	Gfap$^+$ non-myelinating Schwann cells associated with nerve fibers tend to localize in the central BM.	NA	Indirect evidence of an HSC-niche supporting role by neural crest lineage cells	(Acar et al., 2015)
8w-12w	*NG2*-CreER$^+$ cells	►Not detected in *Scf*-GFP$^+$ or Cxcl12-DsRed$^+$ cells ►*NG2*-CreER mediated conditional deletion of Scf in Scf$^{GFP/fl}$ mice or Cxcl12 in *NG2*–CreER: Cxcl12$^{-/fl}$ mice did not affect HSC frequency.	NA	*Nes*-Cre mediated deletion of *Scf* also shows no effects on HSC function (Ding et al. 2012).	(Acar et al., 2015)
8w-12w	HSCs	Higher HSC density, marked by α-catulin-GFP$^+$/c-kit$^+$, found in the diaphysis than in metaphysis	NA	An unexpected result that might provide insights into HSC niche dynamics	(Acar et al., 2015)
8w-16w	BM stromal cells	CD45$^-$/Ter119$^-$ non-hematopoietic BM cells	1.4%	None	(Zhou et al., 2014)
8w-16w	PDFFRα+	PDGFRα$^+$/CD45$^-$/Ter119$^-$ BM stromal cells	10%	None	(Zhou et al., 2014)
8w-16w	PDFFRα$^+$ /Sca-I$^+$	The PDGFRα$^+$/Sca-1$^+$/CD45$^-$/Ter119$^-$ cell population	16%	Reside mainly around arterioles, but does not express the HSC niche factor Cxcl12	(Zhou et al., 2014)
8w-16w	PDFFRα$^+$ /Sca-1$^-$	The PDGFRα$^+$/Sca-1$^-$/CD45$^-$/Ter119$^-$ cell population, known as CXCL12-abundant reticular (CAR) cells	8%	Exist primarily around sinusoids and express high levels of Cxcl12	(Zhou et al., 2014)
8w-16w	*Lepr*-Cre /Tomato$^+$ /CD105$^+$	►0.3% *Lepr*-Cre$^+$/CD45$^-$/Ter119$^-$ cells ►98% PDFFRα$^+$, 98% CD51$^+$, 69% CD105$^+$ ►Around sinusoids and arterioles ►High levels of *Lepr* mRNAs ►The Lepr protein detected by immunostaining ►Considered as a major source of BM SSCs	14%	►Tripotent cells from 9% of CFU-F colonies ►Ossicles from 30% CFC-F colonies ►CD105, known as endoglin, a plasma membrane and extracellular glycoprotein of vascular endothelial cells, used as an “MSC” marker	(Zhou et al., 2014)
8w-16w	*Lepr*-Cre /Tomato$^-$ CD105$^-$	*Lepr*-Cre/Tomato$^-$/CD105$^-$/CD45$^-$/Ter119$^-$ BM stromal cells	1%	14-fold decrease in CFU-F colonies compared with *Lepr*-Cre/Tomato$^+$ /CD105$^+$ cells	(Zhou et al., 2014)
8w-16w	*Lepr*-Cre /Tomato$^+$	*Lepr*-Cre/Tomato$^+$/CD45$^-$/Ter119$^-$ BM stromal cells	11%	Around sinusoids and arterioles	(Zhou et al., 2014)
8w-16w	*Lepr*-Cre/Tomato$^-$	*Lepr*-Cre/Tomato$^-$/CD45$^-$/Ter119$^-$ BM stromal cells	0.1%	Depletion of CFU-F capacity	(Zhou et al., 2014)
8w-16w	*Lepr-Cre*$^+$ /Scf-GFP$^+$	*Lepr*-Cre/Tomato$^+$/*Scf*-GFP$^+$/CD45$^-$ /Ter119$^-$ BM stromal cells	NA	Around sinusoids only	(Zhou et al., 2014)
8w-16w	*Prx1*-Cre /Tomato$^+$	*Prx1*-Cre/Tomato$^+$/CD45$^-$/Ter119$^-$ BM stromal cells	10%	A positive marker for BM stromal cells, tightly associated with *Lepr*-Cre	(Zhou et al., 2014)
8w-16w	*Scf*-GFP$^+$	*Scf*-GFP$^+$/CD45$^-$/Ter119$^-$ BM stromal cells	10%	A positive marker for BM stromal cells	(Zhou et al., 2014)
8w-16w	Cxcl12-DsRed^{high}	Cxcl12-DsRed^{high}/CD45$^-$/Ter119$^-$ BM stromal cells	12%	A positive marker for BM stromal cells	(Zhou et al., 2014)
8w-16w	*Nes*-GFP^{low}	*Nes*-GFP^{low}/CD45$^-$/Ter119$^-$ BM stromal cells	8%	A positive marker for BM stromal cells	(Zhou et al., 2014)
8w-16w	*Nes*-GFP^{high}	*Nes*-GFP^{high}/CD45$^-$/Ter119$^-$ BM stromal cells	3%	See comments on *NG2*-CreER$^+$ cells	(Zhou et al., 2014)
8w-16w	*Nes*-CreER$^+$	*Nes*-CreER$^+$/CD45$^-$/Ter119$^-$ BM stromal cells	0	A negative marker for BM stromal cells	(Zhou et al., 2014)

8w-16w	*NG2*-CreER^{+}	*NG2*-CreER^{+}/CD45^{-}/Ter119^{-} BM stromal cells	2%	*NG2*-Cre^{+} and *Nes*-GFP^{+} cells show similar low CFU-F activity.	(Zhou et al., 2014)
8w-16w	*Mx1*-CreER^{+}	*Mx1*-CreER^{+}/CD45^{-}/Ter119^{-} BM stromal cells	2%	*Mx1*-Cre seems a weaker marker for osteoblastic lineage at this stage.	(Zhou et al., 2014)
12w-16w	*Prx1*-Cre; Jak2^{V617F}	►Jak2 mutant cells had a 3-fold decrease in CFU-F activity compared with the wild-type cells. ►Increase in adipocytes	Low	Genetic evidence indicates Jak2/Stat3 is underlying the regulation of both adipogenesis and osteogenesis.	(Yue et al., 2016)
12w-16w	*Nes*-creER^{T2}: RCE-loxP	Pulsed with tamoxifen at 3 months and chased for 4w (1 month): No *Nes*-Cre^{+} osteoblasts, osteocytes, and chondrocytes (collagen α1 type 2^{+})	NA	*Nes*-Cre mediates slow turnover of osteolineage cells.	(Mendez-Ferrer et al., 2010)
12w-44w	*Nes*-creER^{T2}: RCE-loxP	Pulsed with tamoxifen at 3 months (12w) and chased for 8 months (44w): see GFP^{+} osteoblasts, osteocytes, and chondrocytes (collagen α1 type 2^{+})	NA	Adult *Nes*-Cre^{+} cells are likely an SSC source.	(Mendez-Ferrer et al., 2010)
15w	*Lepr*-Cre^{+} cells	Distributed not only in the BM cavity, but also along the cortical bone as *Lepr*-/Cre^{+}/Ocn^{+}/DMP1^{+} osteoblasts and osteocytes	NA	This study suggests a migration route of *Lepr*-Cre^{+} cells during osteogenesis: BM cavity → endosteum → trabecular bone → cortical bone.	(Mizoguchi et al., 2014)
24w	*Prx1*-Cre /*Lepr*$^{fl/fl}$	Conditional deletion of *Lepr* in SSCs: increased osteogenesis and down-regulated adipogenesis	NA	The Lepr protein is likely an inhibitor of adult osteogenesis.	(Yue et al., 2016)
24w, 40w, 56w	*Lepr*-Cre: dTomato: *Col2.3*-GFP	Age-dependent contribution of *Lepr*-Cre^{+} cells to bone development: 24w: 10%–23% of *Col2.3*-GFP^{+} cells, 40w: 43%–67% of *Col2.3*-GFP^{+} cells, 56w: 61%–81% of *Col2.3*-GFP^{+} cells	NA	Accordingly, no Lepr protein expression was detected by IF (at 10m or 40w), which suggests that *Lepr*-Cre functions as an independent transcriptional reporter in these stages	(Zhou et al., 2014)

ABBREVIATIONS:

Adrb3, β3 adrenoreceptor; BM, bone marrow; CFU-F, Colony forming unit-fibroblastic, an assay based on freshly isolated single cells from an intact tissue, in which single cells are able to initiate clonal growth of fibroblastic cells at low density; Col1, collagen I; DMP1, dentin matrix protein 1; HSC, hematopoietic stem cell; iDTA, diphtheria toxin; iDTAR, diphtheria toxin receptor; IF, immunofluorescence; m, month(s); MSC, “mesenchymal stem cells”; NA, not available; *Nes*-CreER^{T2}, tamoxifen-inducible transgenic mouse described by Balordi and Fishell (2007); Ocn, osteocalcin; Osx, osterix; POC, primary ossification center; SSC, skeletal stem cell; Tripotent: osteochondrogenic, osteogenic, and adipogenic; wk, week

REREFERNCES

Acar, M., Kocherlakota, K.S., Murphy, M.M., Peyer, J.G., Oguro, H., Inra, C.N., Jaiyeola, C., Zhao, Z., Luby-Phelps, K., and Morrison, S.J. (2015). Deep imaging of bone marrow shows non-dividing stem cells are mainly perisinusoidal. Nature 526, 126-130.

Balordi, F., and Fishell, G. (2007). Mosaic removal of hedgehog signaling in the adult SVZ reveals that the residual wild-type stem cells have a limited capacity for self-renewal. J Neurosci 27, 14248-59.

Ding, L., and Morrison, S.J. (2013). Haematopoietic stem cells and early lymphoid progenitors occupy distinct bone marrow niches. Nature 495, 231-235.

Isern, J., García-García, A., Martín, A.M., Arranz, L., Martín-Pérez, D., Torroja, C., Sánchez-Cabo, F., Méndez-Ferrer, S. (2014). The neural crest is a source of mesenchymal stem cells with specialized hematopoietic stem cell niche function. Elife 25; 3:e03696.

Kunisaki, Y., Bruns, I., Scheiermann, C., Ahmed, J., Pinho, S., Zhang, D., Mizoguchi, T., Wei, Q., Lucas, D., Ito, K., et al. (2013). Arteriolar niches maintain haematopoietic stem cell quiescence. Nature 502, 637-643.

Mendez-Ferrer, S., Michurina, T.V., Ferraro, F., Mazloom, A.R., Macarthur, B.D., Lira, S.A., Scadden, D.T., Ma'ayan, A., Enikolopov, G.N., and Frenette, P.S. (2010). Mesenchymal and haematopoietic stem cells form a unique bone marrow niche. Nature 466, 829-834.

Mizoguchi, T., Pinho, S., Ahmed, J., Kunisaki, Y., Hanoun, M., Mendelson, A., Ono, N., Kronenberg, H.M., and Frenette, P.S. (2014). Osterix marks distinct waves of primitive and definitive stromal progenitors during bone marrow development. Dev Cell 29, 340-349.

Ono, N., Ono, W., Mizoguchi, T., Nagasawa, T., Frenette, P.S., and Kronenberg, H.M. (2014). Vasculature-associated cells expressing nestin in developing bones encompass early cells in the osteoblast and endothelial lineage. Dev Cell 29, 330-339.

Park, D., Spencer, J.A., Koh, B.I., Kobayashi, T., Fujisaki, J., Clemens, T.L., Lin, C.P., Kronenberg, H.M., and Scadden, D.T. (2012). Endogenous bone marrow MSCs are dynamic, fate-restricted participants in bone maintenance and regeneration. Cell Stem Cell 10, 259-72.

Pinho, S., Lacombe, J., Hanoun, M., Mizoguchi, T., Bruns, I., Kunisaki, Y., and Frenette, P.S. (2013). PDGFRalpha and CD51 mark human nestin+ sphere-forming mesenchymal stem cells capable of hematopoietic progenitor cell expansion. J Exp Med 210, 1351-1367.

Yue, R., Zhou, B.O., Shimada, I.S., Zhao, Z., and Morrison, S.J. (2016). Leptin Receptor Promotes Adipogenesis and Reduces Osteogenesis by Regulating Mesenchymal Stromal Cells in Adult Bone Marrow. Cell Stem Cell 18, 782-796.

Zhou, B.O., Yue, R., Murphy, M.M., Peyer, J.G., and Morrison, S.J. (2014). Leptin-receptor-expressing mesenchymal stromal cells represent the main source of bone formed by adult bone marrow. Cell Stem Cell 15, 154-168.

Figure S1

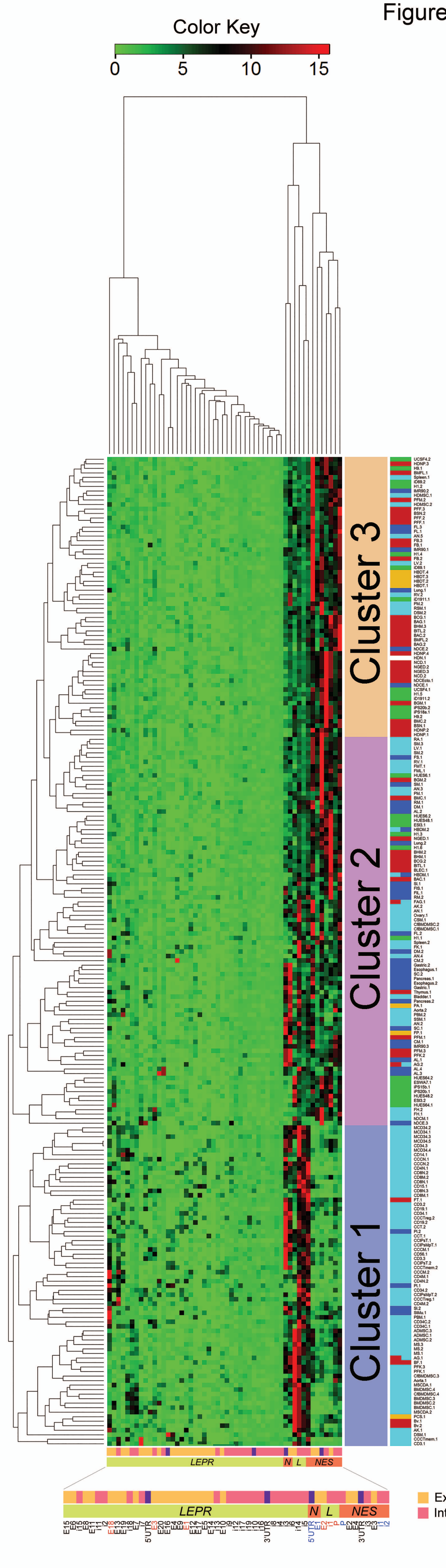
Color Key
0
5
10
15
Cluster 3
Cluster 2
Cluster 1
LEPR
N
L
NES
5'UTR
3'UTR
Exon
Intron